Received: 8 October 2019 | Revised: 21 January 2020 | Accepted: 21 January 2020

DOI: 10.1096/fj.201902557RRR

RESEARCH ARTICLE

THE FASEB JOURNAL

The glucocorticoid-induced leucine zipper mediates statin-induced muscle damage

Jessica Hoppstädter[1,2] | Jenny Vanessa Valbuena Perez[1] | Rebecca Linnenberger[1] | Charlotte Dahlem[1] | Thierry M. Legroux[1] | Anne Hecksteden[3] | William K. F. Tse[4] | Sara Flamini[2] | Anastasia Andreas[5] | Jennifer Herrmann[5] | Christian Herr[6] | Rolf Müller[5] | Tim Meyer[3] | Robert Bals[6] | Carlo Riccardi[2] | Stefano Bruscoli[2] | Alexandra K. Kiemer[1]

[1]Department of Pharmacy, Pharmaceutical Biology, Saarland University, Saarbrücken, Germany

[2]Department of Medicine, Section of Pharmacology, University of Perugia, Perugia, Italy

[3]Institute of Sports and Preventive Medicine, Saarland University, Saarbrücken, Germany

[4]Center for Promotion of International Education and Research, Faculty of Agriculture, Kyushu University, Fukuoka, Japan

[5]Department of Microbial Natural Products, Helmholtz Institute for Pharmaceutical Research Saarland (HIPS), Saarbrücken, Germany

[6]Department of Internal Medicine V—Pulmonology, Allergology and Critical Care Medicine, Saarland University, Homburg, Germany

Correspondence
Alexandra K. Kiemer, Pharmaceutical Biology, Saarland University, Saarbrücken D-66123, Germany.
Email: pharm.bio.kiemer@mx.uni-saarland.de

Abstract

Statins, the most prescribed class of drugs for the treatment of hypercholesterolemia, can cause muscle-related adverse effects. It has been shown that the glucocorticoid-induced leucine zipper (GILZ) plays a key role in the anti-myogenic action of dexamethasone. In the present study, we aimed to evaluate the role of GILZ in statin-induced myopathy**.** Statins induced GILZ expression in C2C12 cells, primary murine myoblasts/myotubes, primary human myoblasts, and in vivo in zebrafish embryos and human quadriceps femoris muscle. *Gilz* induction was mediated by FOXO3 activation and binding to the *Gilz* promoter, and could be reversed by the addition of geranylgeranyl, but not farnesyl, pyrophosphate. Atorvastatin decreased Akt phosphorylation and increased cleaved caspase-3 levels in myoblasts. This effect was reversed in myoblasts from GILZ knockout mice. Similarly, myofibers isolated from knockout animals were more resistant toward statin-induced cell death than their wild-type counterparts. Statins also impaired myoblast differentiation, and this effect was accompanied by GILZ induction. The in vivo relevance of our findings was supported by the observation that *gilz* overexpression in zebrafish embryos led to impaired embryonic muscle development. Taken together, our data point toward GILZ as an essential mediator of the molecular mechanisms leading to statin-induced muscle damage.

Abbreviations: CVD, cardiovascular disease; DM, differentiation medium; FDB, *flexor digitorum brevis*; FHRE, forkhead-responsive element; FPP, farnesyl pyrophosphate; GGPP, geranylgeranyl pyrophosphate; GILZ, glucocorticoid-induced leucine zipper; HMG-CoA, 3-hydroxy-3-methylglutaryl coenzyme A; hpf, hours post fertilization; MHC, myosin heavy chain; MRF, muscle regulatory factor; MTT, 3-(4,5-dimethylthiazol-2-yl)-2,5-diphenyltetrazolium bromide; MVA, mevalonate; SAMS, statin-associated muscle symptoms.

Jessica Hoppstädter and Jenny Vanessa Valbuena Perez equally contributed to this work.

Funding information
Deutsche Forschungsgemeinschaft, Grant/Award Number: KI702; German Academic Exchange Service; Studienstiftung

KEYWORDS
flexor digitorum brevis, HMG-CoA, muscle wasting, statin-associated muscle symptoms, *Tsc22d3*

1 | INTRODUCTION

Statins are the first line of treatment in the management of hyperlipidemia and the prevention of cardiovascular disease (CVD).[1,2] These drugs are inhibitors of the 3-hydroxy-3-methylglutaryl coenzyme A (HMG-CoA) reductase enzyme, preventing the biosynthesis of cholesterol in the liver by blocking the mevalonate pathway and, as a consequence, enhancing clearance of circulating LDL-cholesterol.[3,4] Since their introduction in 1987, statin prescription rates have risen, as shown by several studies in different populations,[5-7] positioning them among the most prescribed drug classes worldwide. Given the high prevalence of CVD and the favorable data on CVD prevention by statins,[8,9] this tendency seems to be maintained.

Statins have a satisfactory safety profile, their most relevant adverse effect being skeletal muscle toxicity.[1] Statin-associated muscle symptoms (SAMS) have an incidence of 5%-29% in clinical practice,[1,10] can range from mild myalgia to, in rare cases, fatal rhabdomyolysis,[11] and are a frequent cause for nonadherence to treatment or its discontinuation.[12] Although several studies have been conducted, and a number of risk factors that contribute to the onset of SAMS have been described, such as sex, pharmacokinetic differences, or genetic factors,[13,14] the molecular mechanisms leading to myopathy are still not fully understood.

The glucocorticoid-induced leucine zipper (GILZ) was first described as a dexamethasone-induced, immunomodulatory protein.[15] Since then, it has been shown that GILZ basal expression is not restricted to immune cells but is extended to several tissues, including skeletal muscle.[16] GILZ plays multiple roles in both glucocorticoid and non-glucocorticoid-mediated cellular processes[17] beyond its immune-modulating function. For instance, studies demonstrated a role for GILZ in inhibition of adipocyte differentiation,[18] in sodium homeostasis in the kidney,[19,20] and in spermatogenesis.[21] Of particular interest is the role described for GILZ in the regulation of skeletal muscle differentiation: GILZ is strongly induced by dexamethasone, mediating its antimyogenic effects *via* inhibition of the transcriptional activity of an early muscle regulatory factor (MRF), MyoD.[22]

In the present study, we aimed to test the hypothesis that GILZ plays a role in the onset of SAMS, focusing on both myotoxic and antimyogenic effects.

2 | MATERIALS AND METHODS

2.1 | Reagents

Cell culture reagents, atorvastatin, simvastatin lactone, cerivastatin, and mevalonic acid lithium salt were obtained from Sigma-Aldrich (St. Louis, MO, USA). The simvastatin sodium salt, geranylgeranyl pyrophosphate (GGPP), and farnesyl pyrophosphate (FPP) were obtained from Cayman Chemicals (Ann Arbour, MI, USA). Statin stock solutions were prepared in DMSO.

2.2 | Cell line

C2C12 cells were maintained in high-glucose DMEM supplemented with 10% FBS, 100 U/mL penicillin, 100 µg/mL streptomycin, and 2 mM glutamine. For inducing differentiation, confluent cell layers were cultured in high-glucose DMEM supplemented with 2% horse serum, penicillin/streptomycin, and glutamine (differentiation medium, DM), with medium change every other day. All cells were cultured at 37°C in a humidified atmosphere with 5% CO_2. For experiments, cells were seeded at a density of 2.5×10^4 cells/cm^2 (or 5×10^4 cells/cm^2 for differentiation).

2.3 | Mice

C57BL/6J mice were housed in a 12/12-hour light/dark cycle with food and water *ad libitum*. GILZ knockout (KO) mice were generated as previously described.[21] Animal care and maintenance were in compliance with regulations in Italy (DL 26/2014) and Europe (EU Directive 2010/63/EU).

2.4 | *Flexor digitorum brevis* (FDB) muscle fibers

FDB fibers were isolated from wild-type (WT) or GILZ KO mice following a protocol adapted from the literature.[23,24] The FDB muscles were dissected under a stereomicroscope and digested in a 0.2% collagenase A solution in DMEM for 60 minutes. Then, the myofibers were carefully separated under a stereo dissecting microscope, dispersed in DMEM containing 10% horse serum by drawing through a series of

pipette tips with gradually decreasing diameter and purified by sedimentation steps. Pure fibers were plated in laminin-coated cell culture dishes and cultured in DMEM supplemented with 20% serum replacement 2, 1% horse serum, penicillin/streptomycin, and glutamine.

2.5 | Primary human myoblasts

Primary human myoblasts (#CC-2580) were obtained from Lonza (Basel, Switzerland) and grown in Skeletal Muscle Growth Medium-2 (SkGM-2 basal medium, Lonza) with supplements (Lonza, #CC-3244 containing human epidermal growth factor, dexamethasone, L-glutamine, FCS, and gentamicin/amphotericin-B) according to the manufacturer's instructions. For experiments, cells were seeded at a density of 1-1.5 $\times$ 10^4 cells/well in SkGM-2 with all supplements except for dexamethasone.

2.6 | Primary murine myoblasts

Primary myoblasts were isolated from hind limbs of male 3-day-old WT or GILZ KO mice. The hind limbs were dissected and shredded with scissors, washed in PBS, and digested with trypsin/EDTA for 60 minutes. After filtering through a 70-µm cell strainer, the cell suspension was diluted in DMEM supplemented with 10% FBS and centrifuged for 20 minutes at 200×*g* and 4ºC. The resuspended cells were preplated for 1 hour to allow fibroblast adhesion. Nonadherent cells were collected, centrifuged for 10 minutes at 200×*g* and 4ºC, resuspended in F-10-based primary myoblast growth medium (Ham's F-10 nutrient mixture supplemented with 20% FBS, penicillin/streptomycin, and glutamine), and plated onto collagen I-coated cell culture dishes (Sigma-Aldrich, St. Louis, MO, USA). Further enrichment of the myoblasts was achieved by dislodging and preplating the cells onto collagen-coated dishes every fourth day for 1-2 weeks. Afterward, myoblasts were cultured in growth medium (40% DMEM, 40% Ham's F-10 nutrient mixture, 20% FBS), supplemented with penicillin/streptomycin and glutamine.

2.7 | Cytotoxicity measurement

For the 3-(4,5-dimethylthiazol-2-yl)-2,5-diphenyltetrazolium bromide (MTT) reduction assay, cells were seeded in 96-well plates at a density of 10^4 cells/well, allowed to adhere overnight, and treated with test compounds at the indicated concentrations. Cells incubated without any treatment were used as growth controls, cells incubated with solvent at the maximum concentration present in the assay (0.25%) served as negative controls, and wells with treatment but without cells were used as blank. At the end of treatment, cells were incubated for 3 hours with MTT solution (0.5 mg/mL in medium) and lysed with DMSO. The absorbance was measured at 550 nm in a microplate reader (XFluor4 SunriseTM, TECAN, Männedorf, Switzerland), using a reference wavelength of 690 nm.

For the crystal violet assays, cells were seeded at a density of 10^4 cells/well into a 96-well plate. After overnight incubation, cells were treated with statins or vehicle control at the indicated concentrations. The cells were washed with PBS and incubated for 20 minutes with 50 µL/well of freshly prepared 0.5% crystal violet solution in water. After washing, the plate was air-dried for 24 hours. Cells were lysed in methanol by incubation for 20 minutes at room temperature. The optical density was measured at 570 nm. The background was determined by lysing cells with 50% DMSO before the staining procedure, and background-subtracted values were used to calculate the cell viability.

For evaluating the cell viability in FDBs, the number of living and nonliving myofibers was determined using the trypan blue exclusion method.

2.8 | RNA isolation, reverse transcription, and quantitative PCR (RT-qPCR)

Total RNA from cultured cells was isolated using the High Pure RNA Isolation Kit (Roche, Basel, Switzerland). RNA samples with an A260/A280 ratio higher than 1.8 were used for further analysis. Reverse transcription was done using the High-Capacity cDNA Reverse Transcription Kit (Thermo Fisher Scientific, Waltham, MA, USA) in the presence of RNase inhibitor (Thermo Fisher Scientific, Waltham, MA, USA). qPCR was performed on cDNA samples using the 5×HotFirePol EvaGreen qPCR Mix (Solis BioDyne, Tartu, Estonia) and the primer sequences detailed in Table 1. A CFX96 touch Real-Time PCR detection system, and the CFX Manager 2.1 software (Bio-Rad, Hercules, CA, USA) were used for qPCR analysis. Data were analyzed as previously described.[25] Housekeeping genes were chosen based on the literature, or after evaluating the expression stability of at least three candidate genes under the experimental conditions, using the geNorm, NormFinder, and BestKeeper software tools.[26]

2.9 | Western blot

Cells were harvested either with RIPA buffer (50 mM Tris-HCl, 1% Triton X-100, 0.1% SDS, 0.5% sodium deoxycholate, 150 mM NaCl) supplemented with a protease/phosphatase inhibitor mix (P8340, P0044, Sigma-Aldrich,

TABLE 1 Primer sequences for qPCR analyses

Gene	Accession number	Forward primer sequence 5´-3´	Reverse primer sequence 5´-3´
Mouse			
Csnk2a2	NM_009974.3	GTAAAGGACCCTGTGTCAAAGA	GTCAGGATCTGGTAGAGTTGCT
Ppia	NM_008907.1	GCGTCTCCTTCGAGCTGTTT	CACCCTGGCACATGAATCCT
Hmgcr	NM_008255.2	ATCCAGGAGCGAACCAAGAGAG	CAGAAGCCCCAAGCACAAAC
Tsc22d3	NM_010286.4	GCTGCTTGAGAAGAACTCCCA	GAACTTTTCCAGTTGCTCGGG
Human			
RNA18S5	NR_003278.3	AGGTCTGTGATGCCCTTAGA	GAATGGGGTTCAACGGGTTA
TSC22D3	NM_004089.3	CATGTGGTTTCCGTTAAGCTGG	AGGATCTCCACCTCCTCTCTC
Zebrafish			
actb2	NM_181601.4	AAATTGCCGCACTGGTT	ACGATGGATGGGAAGACA
tsc22d3	NM_200569.2	AACAACCAGCTGGAGCGCGAA	GCAGAGCCCGTGCTGCTGTATT

St. Louis, MO, USA) or with SB lysis buffer (50 mM Tris-HCl, 1% SDS, 10% glycerol, 5% β-mercaptoethanol, 0.004% bromophenol blue, in water) supplemented with a protease inhibitor cocktail (cOmplete Mini, Roche, Basel, Switzerland). Western blots were performed as described previously, and signals were either detected by an HRP-based method[27] or with the LI-COR Odyssey imaging system (LI-COR Biosciences, Lincoln, NE, USA) .[28,29] Incubation with primary antibody dilutions was performed at 4°C overnight, and with secondary antibody dilutions at room temperature for 1-1.5 hours. The antibodies and dilutions used are listed in Table 2.

2.10 | Jenner-Giemsa staining

To measure the myogenic differentiation of C2C12 myotubes Jenner-Giemsa staining was performed following a previously published protocol.[30] In brief, cells were fixed in ice-cold methanol for 5 minutes, air-dried, and stored at 4°C until analysis. For staining, wells were incubated with Jenner's stain solution (diluted 1:3 in 1 mM sodium phosphate buffer pH 5.6) for 5 minutes at room temperature, washed with distilled water, and subsequently incubated with Giemsa solution (diluted 1:20 in the same buffer) for 10 minutes at room temperature. Wells were observed with a phase-contrast microscope equipped with a digital camera (ZEISS Axiovert 40 CFL with Canon EOS 400D, Oberkochen, Germany). Each well was photographed in 3-4 randomly selected regions. Images were analyzed using the free image-processing software Fiji (*Fiji is just ImageJ*) .[31]

2.11 | Immunofluorescence

Myosin heavy chain (MHC) immunofluorescence (IF) was performed on C2C12 myotubes and whole zebrafish embryos. Cells were cultured and differentiated on glass coverslips that were previously treated for 10 minutes in a 1:1 mixture of 70% ethanol and 0.1 N HCl.[32] Cells were treated as indicated and prefixed by adding paraformaldehyde solution (4% in PBS) directly to the culture medium. After 2 minutes, the prefixation culture medium was replaced with a paraformaldehyde solution (4% in PBS), and cells were fixed for 15 minutes at room temperature. Cells were washed with PBS and permeabilized with a 0.2% Triton X-100 solution in PBS for 10 minutes at room temperature, washed, blocked in a 5% BSA solution in PBS for 1 hour at room temperature, and incubated with primary antibody (MF20, deposited by Donald A. Fischman in the Developmental Studies Hybridoma Bank, The University of Iowa, Department of Biology, Iowa City, IA, USA) diluted 1:50 in dilution buffer (1% BSA in PBS) at 4°C overnight. After washing, cells were incubated with secondary antibody diluted 1:800 in dilution buffer for 1 hour at room temperature. Cells were washed and counterstained with DAPI for 15 minutes at room temperature, mounted with FluorSave (Merck, Darmstadt, Germany), and observed with an Axio Observer Z1 epifluorescence microscope, equipped with an AxioCam Mr3 and AxioVision software (Zeiss, Oberkochen, Germany). Photographs from randomly selected regions were analyzed using the Fiji software.

Zebrafish embryos were fixed in paraformaldehyde solution at 4°C overnight, and then stored in methanol at −20°C for at least 4 hours. Embryos were permeabilized in acetone for 30 minutes at −20°C, washed, blocked in a 1% BSA solution in PBST for 2 hours at room temperature, and incubated with primary antibody (mouse anti-myosin F59, DSHB, Iowa City, IA) diluted 1:100 in blocking buffer at 4°C overnight. After washing in PBST, the embryos were incubated with secondary antibody (goat anti-mouse IgG (H+L), Alexa Fluor 597, Thermo Fisher Scientific, Waltham, MA, USA) 1:200 at room temperature for 4 hours, washed again, and observed on a Leica SP8 confocal microscope.

TABLE 2 Antibodies for Western blot analyses

Antibody	Dilution
Rat anti GILZ [CFMKG15] mAb (Thermo Fisher Scientific, Waltham, MA, USA)	For detection with HRP-labeled secondary antibodies: 1:1000 in 5% milk powder—TBST For detection with IR-labeled secondary antibodies: 1:1000 in Rockland blocking buffer (Rockland, Limerick, PA, USA)
Mouse anti GADPH [OTI2D9] (OriGene, Rockville, MA, USA)	1:2000 in 5% milk powder—TBST
Mouse anti Akt (pan) [40D4] mAb (New England Biolabs, Ipswich, MA, USA)	1:2000 in 5% milk powder—TBST
Rabbit anti phospho-Akt (Ser473) [D9E] XP® mAb (New England Biolabs, Ipswich, MA, USA)	1:2000 in 5% milk powder—TBST
Polyclonal rabbit anti phospho-FOXO3a (Ser253) (New England Biolabs, Ipswich, MA, USA)	1:2000 in 5% milk powder—TBST
Mouse anti FOXO3a [D12] mAb (Santa Cruz Biotechnology, Dallas, TX, USA)	1:1000 in gelatine buffer (0.75% gelatine A , 0.1% Tween-20, 20 mM Tris, 137 mM NaCl, pH 7.5)
Mouse anti myogenin [5FD] mAb (Santa Cruz Biotechnology, Dallas, TX, USA)	1:200 in 5% milk powder—TBST
Polyclonal rabbit anti cleaved Caspase-3 (Cell Signaling Technology, Beverly, MA, USA)	1:1000 in 5% milk powder—TBST
Goat anti-rat IgG (H+L), HRP (Thermo Fisher Scientific, Waltham, MA, USA)	1:5000 in 5% milk powder—TBST
Goat anti-mouse IgG (H+L), HRP (Thermo Fisher Scientific, Waltham, MA, USA)	1:5000 in 5% milk powder—TBST
Goat anti-rabbit IgG, HRP (Thermo Fisher Scientific, Waltham, MA, USA)	1:10 000 in 5% milk powder—TBST
Mouse anti-α-Tubulin [DM1A] (Sigma-Aldrich, St. Louis, MO, USA)	1:1000 in Rockland blocking buffer
IRDye 800CW Goat anti-Rat IgG (LI-COR Biosciences, Lincoln, NE, USA)	1:10 000 in Rockland blocking buffer

2.12 | Zebrafish treatment

Zebrafish embryos from the AB wild-type strain were used. The developmental stage was determined by embryo morphology in hours post fertilization (hpf).[33] To examine gene expression after statin treatment, embryos at 19-22 hpf were sorted, placed at a density of 2-3 embryos/cm^2 in 6-well plates, and incubated at 28°C in 0.3 × Danieau's solution (17 mM NaCl, 2 mM KCl, 1.5 mM HEPES, 1.8 mM $Ca(NO_3)_2$, 0.12 mM $MgSO_4$) containing 1 μM statin or solvent control. 12 hours after treatment, 10-20 embryos were pooled, flash-frozen in liquid nitrogen, and stored at −80°C for RNA isolation and qPCR analysis. To analyze muscle development and movement of the embryos, *gilz* was overexpressed in zebrafish embryos by injecting 1200 pg RNA into 1-2 cell stage embryos.[34] RNA was generated using the pCS2+ construct. Statin treatment was performed by injection of 1-ng statin (equal to 1/2 of the daily human dose related to body weight) into the embryos in the 1-2 cell stage.

The morpholino antisense oligonucleotides (MO) were purchased from Gene Tools (Philomath, OR, USA). To knockdown *foxo3b*, a splicing MO (*foxo3b* MO 5′-TGGAGATGCACTGCGCTTACCTTCC-3′) targeting exon 2 and intron 2 was used as previously described.[35] The Gene Tools random control oligo was used for comparison. MOs were dissolved in sterile water, and 1 nL containing 16 ng MO were injected into 1-2 cell stage embryos. The knockdown was validated by detection of truncated PCR products in *foxo3b* morphants as described.[35] The used primers were: *foxo3b* forward GTGAGTTACTGCTGGTGATGC (exon 1) and *foxo3b* reverse CACCACGAGCTCTTTCCAGT (exon 3).

2.13 | In situ hybridization

Whole-mount *in situ* hybridization was used to analyze MyoD expression changes in zebrafish embryos. Embryos at 16 hpf were collected and fixed in 4% PFA solution at 4°C overnight. *In situ* hybridization was performed as previously described.[32] In brief, dechorionated embryos were treated with 5 μg/μL proteinase K in PBST for 5 minutes, washed and incubated for 1 hour in hybridization buffer (50% formamide, 5× SSC, 0.1% Tween 20, 1 mg/mL yeast torula RNA, 50 μg/mL heparin) at 65°C. Subsequently, an antisense digoxigenin-labeled RNA probe was added, and the samples were incubated overnight. On the next day, embryos were washed, blocked for 1 hour (5% goat serum in PBST) and incubated with anti-DIG antibody (#11093274910, 1:5000, Roche, Basel, Switzerland) at 4°C overnight. Embryos were washed in AP buffer (100 mM Tris-HCl, 50 mM $MgCl_2$, 100 mM NaCl, 0.1% Tween20), and incubated with staining buffer (0.5% nitroblue tetrazolium, 0.375% 5-bromo-4-chloro-3-indolyl phosphate in AP buffer) in the dark for 30

minutes. Once the pattern appeared, embryos were washed, and 4% PFA was added for at least 20 minutes before embryos were analyzed under the microscope. Scoring was performed according to the following criteria: regular phenotype—parallel somites of same length, V-shaped, homogenous MyoD expression; mild phenotype—irregular somite formation, different lengths, line shaped, somites show less homogenous MyoD expression; severe phenotype: no clear somite formation, different lengths, line shaped, reduced and diffuse MyoD expression.

2.14 | Chromatin immunoprecipitation (ChIP)

The ChIP assay was performed using the EZ-ChIP Kit (Merck, Darmstadt, Germany) according to the manufacturer's instructions. Precleared lysates from 1×10^6 myoblasts in a volume of 100 µL were incubated overnight at 4°C with 10 µg monoclonal anti-FOXO3 antibody (D12, Santa Cruz Biotechnology, Dallas, TX, USA) or 10 µg normal mouse IgG (Merck, Darmstadt, Germany). Immunocomplexes were purified, and qPCR analysis was performed using the SYBR Select Master Mix (Thermo Fisher Scientific, Waltham, MA, USA) and the Applied Biosystems 7300 qPCR system (Foster City, CA, USA). Primer sequences are given in Table 3.

2.15 | Luciferase gene reporter assay

Reporter gene assays were performed as previously described.[25] The proximal *Gilz* promoter (a fragment located between −1938 bp upstream and +206 bp downstream of the transcription start site) was cloned into the pGL3 luciferase reporter vector (Promega, Madison, WI, USA) using KpnI and SmaI according to the manufacturer's instructions. The FOXO3 reporter vector (FHRE-Luc) was a gift from Michael Greenberg (Addgene plasmid #1789).[36] The phRG-TK vector (Promega, Madison, WI, USA) provided constitutive expression of *Renilla* luciferase and served as an internal control value, to which expression of the firefly luciferase reporter gene was normalized. C2C12 cells were seeded at a density of 10^4 cells/well into 96-well plates, co-transfected in a 1:1 ratio with the luciferase vector using the Lipofectamine 3000 reagent (Thermo Fisher Scientific, Waltham, MA, USA) for 4 hours, treated as indicated, and harvested by the addition of 1× passive lysis buffer (Promega, Madison, WI, USA). Luciferase activity was determined by the addition of firefly luciferase substrate (470 µM D-luciferin, 530 µM ATP, 270 µM coenzyme A, 33 µM DTT, 20 µM Tricine, 2.67 µM $MgSO_4$, 1.07 µM $MgCO_3$, and 0.1 µM EDTA, pH 7.8) or renilla substrate solution (0.1 M NaCl, 25 mM Tris HCl pH 7.5, 1 mM $CaCl_2$, and 0.9 µM coelenterazine) followed by luminescence measurement using the Glomax Discover multiplate reader (Promega, Madison, WI, USA).

2.16 | Lentivirus preparation

Plasmids encoding lentiviral products were obtained from Addgene (Watertown, MA, USA). The packaging plasmid psPAX2 and the envelope plasmid pMD2.G were a gift from Didier Trono (Addgene plasmids #12260 and #12259). The pLKO.1-TRC cloning vector was a gift from David Root (Addgene plasmid #10878).[37] pLKO.1-scrambled shRNA was a gift from David Sabatini (Addgene plasmid #1864).[38]

Two different sequences of short hairpin (sh) RNA targeting murine GILZ were used: shGILZ1 (5′-GGAGTACTGA CTGGTCTCTTA-3′), and shGILZ2 (5′-ACAGCTTCACCT GACAATG-3′). shGILZ sequences were cloned into the pLKO.1-TRC cloning vector. In brief, the cloning vector was double digested with AgeI-HF and EcoRI-HF and purified from an agarose gel. The annealed oligos were then ligated into the vector using T4 DNA ligase overnight at room temperature. The ligation mix was transformed into GT116 *E. coli* (Invivogen, Toulouse, France), and ampicillin-resistant clones were screened for inserts by sequencing using the pLKO.1 sequencing primer.

Lentiviral particles were produced following Addgene's protocol. Briefly, 5×10^5 HEK-293T cells were plated into 6-cm cell culture dishes in medium without antibiotics and transfected at 50%-80% confluency with the transfer, packaging and envelope plasmids (1000:750:250) using the FuGENE 6 Transfection Reagent (Promega, Madison, WI, USA). Twelve to 15 hours after transfection, the medium was replaced with DMEM. The lentivirus-containing media were

TABLE 3 Primer sequences for ChIP experiments

	Forward primer sequence 5´-3´	Reverse primer sequence 5´-3´
FHRE1	TGGCCCAGTTAAACCACATCC	GCTGAACTGTTTACAGTCCCTGA
FHRE2	TAACCGTGTAAACAGGAGCCAG	GGAACTCCTGGGGAAATCCTA
FHRE3	AGCATGGGCAGAAAAAGGAATAAG	CTGGTTTGGTTGGTGTAAACAGT
FHRE4 (IRE, insulin-responsive element)	AGAGCTTTCTTGGTCTGAGAGAAT	AATTTTGAGGTGAGTAGCAGTAGT
non-FHRE	GTATTCGGCCTTCTCCTTGC	CTGCTGCGTGGTGAAAAACA

then harvested at 24 and 48 hours, pooled, centrifuged at 200×*g* for 5 minutes, aliquoted, and stored at −20°C.

To determine the lentiviral titer, viral genomic RNA was purified from 200 µL of freshly harvested lentivirus stock using the High Pure Viral RNA Kit (Roche, Basel, Switzerland). After digestion of residual DNA, 10-fold serial dilutions of the purified viral RNA were reverse transcribed and amplified *via* qPCR, using primers for the 5′LTR region (forward 5′-AGCTTGCCTTGAGTGCTTCA-3′, reverse 5′-TGA CTAAAAGGGTCTGAGGGA-3′), and the 5′ end of the *gag* gene (forward 5′-GGAGCTAGAACGATTCGCAGTTA-3′, reverse 5′-TGTAGCTGTCCCAGTATTTGTC-3′). The copy number (viral particles, VP) contained in the supernatant was calculated from comparison against a plasmid standard curve, and the titer calculated as viral particles per ml of supernatant (VP/mL). Biological titration of the vectors was performed *via* limiting dilution, and for each lentivirus, the ratio from biological to nonbiological titer was established and used for estimation of the functional titer (TU/mL) for all further preparations that were only titrated via the gRNA method. This titer was then used to determine the volume of viral supernatant needed for infecting cells at a given multiplicity of infection (MOI).

2.17 | Generation of C2C12^{shGILZ} stable cell lines

Stable, polyclonal C2C12 cell lines were generated by reverse transducing 7.5×10^4 cells in 6-well plates with scrambled shRNA, shGILZ1, or shGILZ2 lentiviral particles at an MOI of 10 in the presence of polybrene, following the protocol for the generation of stable cell lines available from Addgene (Watertown, MA, USA). Twenty-four hours after transduction, the medium was changed, and 48 hours after infection puromycin (2 µg/mL) was added to select for transduced cells. The puromycin-resistant cells were expanded for 2-3 weeks, after which they were harvested for analysis of gene and protein expression. Further culture and experiments were done in 1 µg/mL puromycin-containing medium. A nontransduced control was run in parallel to confirm that no viable cells were present after selection.

2.18 | Muscle biopsies and sample preparation

Two percutaneous muscle biopsies from the *musculus vastus lateralis* were obtained from a hypercholesteremic volunteer to determine GILZ baseline expression levels. After the onset of simvastatin treatment (40 mg/d), biopsies were obtained after 1-3 months. Semi-automatic needle biopsies were alternately performed on the right and left legs of the participant using the Bard Magnum device with a 12-G disposable needle (C.R. Bard Gm bH, Karlsruhe, Germany). Local anesthesia of the skin and subcutaneous tissue was performed according to standard procedures using Lidocaine as an anesthetic. Muscle samples were immediately frozen in liquid nitrogen and stored at −80°C. Skeletal muscle biopsy samples were mechanically homogenized using a Precellys homogenizer (Bertin Corp., Rockville, MD, USA). RNA was isolated using the miRNeasy Micro Kit according to the manufacturer's instructions (Qiagen, Venlo, Netherlands). Reverse transcription and quantitative PCR was performed as described above.

2.19 | Statistics

Results are expressed as means of at least three independent experiments performed in replicates ± SEM (standard error of the mean). Statistically significant differences between means were determined using the GraphPad Prism 6.0 or Origin 2018b software. An unpaired *t* test was performed for the comparison of two groups, and the comparison of three or more groups was carried out by one or two-way analysis of variance (ANOVA) followed by Bonferroni's post hoc analysis for individual differences. For MTT results F values and degrees of freedom were indicated. A comparison between medians was performed with Kruskal-Wallis test followed by Dunn's post hoc analysis. For categorical data, the chi-squared test was used. Results were considered significant at $P < .05$.

3 | RESULTS

3.1 | GILZ expression in human muscle biopsies

To investigate the potential effect of statin treatment on *GILZ* expression, we analyzed different publicly available gene expression profiling data sets. Gene Expression Omnibus (GEO) data sets GDS2987, GSE32547, and GSE4883 suggested that statins were able to induce *GILZ* in human endothelial cells, human pulmonary artery smooth muscle cells, human umbilical vein endothelial cells, and human peripheral blood monocytes (Supplemental Figure 1). Interestingly, statins also induced *GILZ* in a clinical setting: The analysis of a transcriptional profile of human quadriceps femoris muscle following statin treatment suggested a moderate increase in *GILZ* expression in biopsies from 12 patients receiving atorvastatin and simvastatin for 8 weeks, compared with those receiving placebo (ArrayExpress dataset E-TABM-116, Figure 1).[39] These results were in accordance with increased *GILZ* mRNA levels observed in muscle biopsies from a hypercholesterolemic volunteer after simvastatin treatment (Supplemental Figure 2).

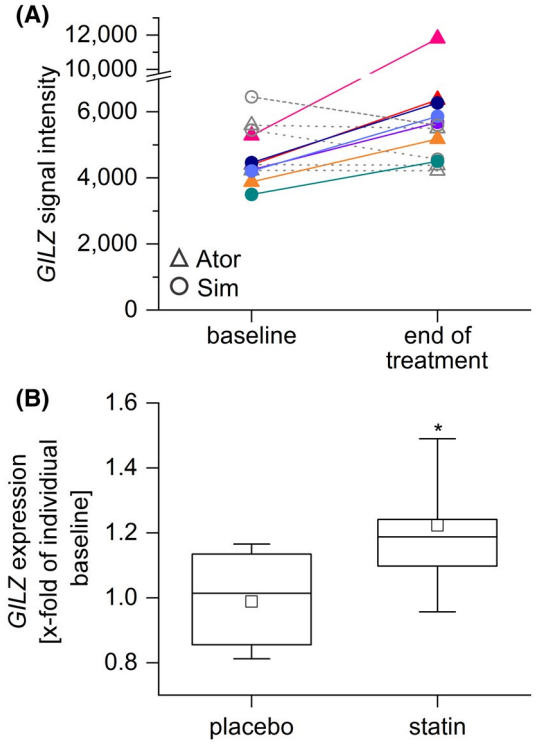

FIGURE 1 Analysis of the publicly available ArrayExpress dataset E-TABM-116: transcription profiling of human quadriceps femoris muscle following simvastatin (80 mg/d) and atorvastatin (40 mg/d) treatment. A, *GILZ* signal intensities (NCBI RefSeq NM_004089.3; scan REFs GI_37622900-A, GI_37622900-I) are shown. Connected data points represent patients before and after intervention for 8 weeks. B, *GILZ* expression after intervention is presented as x-fold of individual baseline levels. Boxplots show the 25-75th percentiles, mean (square), median (line) and SD (whiskers). Placebo group: n = 6, statin group: n = 12. $*P < .05$

3.2 | Toxic concentrations of statin induce GILZ expression in muscle cells

To evaluate whether statins were able to induce GILZ in skeletal muscle cells, we treated C2C12 myoblasts and myotubes with 50 μM atorvastatin, simvastatin, or cerivastatin. These relatively high statin concentrations are in accordance with the literature[34,40-43] and were also chosen based on our observation that C2C12 myoblasts in cell culture express a 50-fold higher *Hmgcr* baseline level compared to muscle in vivo (Supplemental Figure 3). Statins were toxic after 24 hours—but not after 6 hours—at this concentration, as determined by MTT and crystal violet assay (Supplemental Figure 4). We detected an increase in *Gilz* mRNA expression in C2C12 myoblasts and primary human myoblasts after 6 hours of treatment with all statins, which was reversed by the addition of mevalonate (100 μM) to the medium, indicating that the mechanism of GILZ induction relates to the inhibition of HMG-CoA reductase (Figure 2A). In C2C12 myotubes, the increase in *Gilz* expression was less pronounced (Figure 2A). Western blot analysis showed an elevated expression of GILZ protein in C2C12 myoblasts as well as in primary murine and human myoblasts treated with toxic concentrations of statins (Figure 2B-D).

3.3 | GILZ induction can be reversed by geranylgeranyl pyrophosphate

The inhibition of HMG-CoA by statins does not only impair cholesterol biosynthesis, but also other biosynthetic pathways. Of main importance is the inhibition of protein prenylation resulting from the decreased synthesis of the isoprenoid derivatives GGPP and FPP. Thus, we evaluated whether GILZ induction could be reversed by the addition of any, or both, of these mediators to the medium. Co-treatment of C2C12 myoblasts with 10 μM GGPP in addition to simvastatin completely reversed *Gilz* induction, while FPP had no effect (Figure 2E). GGPP treatment alone did not affect *Gilz* expression (data not shown).

3.4 | Statin-induced impairment of myogenesis is accompanied by GILZ induction

Myogenesis is a multistep, tightly regulated process that leads to the formation of skeletal muscle, both during embryonic development as well as in adult life, to maintain muscle homeostasis and repair after injury.[44] Statins are not only toxic toward skeletal muscle fibers but might also impair the muscle regeneration process.[45-47] To examine these effects, we induced the differentiation of C2C12 myoblasts in the absence or presence of statins and evaluated myotube formation by Jenner-Giemsa staining and myosin heavy chain immunofluorescence. We observed that treatment of C2C12 cells with subtoxic concentrations of statins during differentiation resulted in less myotube formation and a significantly reduced fusion index after 6 days, where fully differentiated myotubes were visible in the control (Figure 3A-C). We analyzed GILZ expression levels in differentiating C2C12 and primary murine myotubes treated with statins and found that the impairment in myogenesis was accompanied by GILZ induction on both mRNA and protein level (Figure 3D,E). Since GILZ has been shown to mediate the antimyogenic effects of dexamethasone,[22] we hypothesized that it might also be involved in the effects observed after statin treatment.

3.5 | GILZ knockout abolishes the cytotoxic effects of statins

To assess whether loss of GILZ could rescue statin-induced cytotoxicity, we isolated primary myoblasts from wildtype

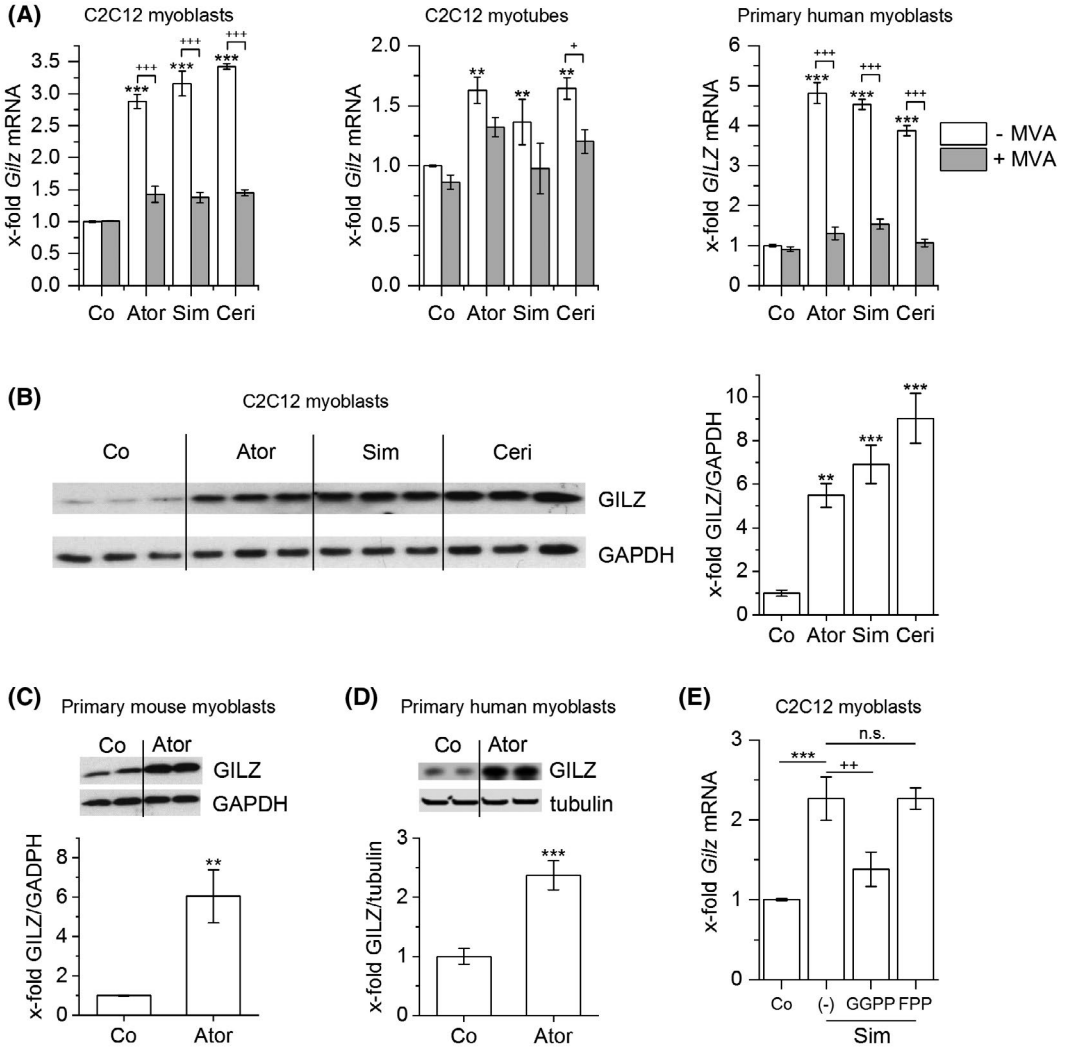

FIGURE 2 Effect of statin treatment at toxic concentrations on GILZ expression in muscle cells. A, C2C12 myoblasts, C2C12 72-h myotubes, or primary human skeletal muscle myoblasts were treated with 50 μM statin (Ator, atorvastatin; Sim, simvastatin; Ceri, cerivastatin) in the absence or presence of mevalonate (MVA, 100 μM) for 6 hours, and mRNA levels were determined by qPCR. *Gilz* expression in C2C12 samples was normalized to the housekeeping gene *Csnk2a2*, and *GILZ* expression in human samples was normalized to *RN18S5*. Data are presented as fold change of control. B-D, GILZ protein expression was determined in vehicle- or atorvastatin-treated C2C12 myoblasts (B), primary murine myoblasts (C), and primary human skeletal muscle myoblasts (D) by western blot. Representative blots and densitometric analyses are shown. For densitometric analysis, GILZ signal intensities were normalized to the housekeeping protein GAPDH (B, C) or tubulin (D). E, C2C12 myoblasts were treated with 50 μM simvastatin in the absence or presence of GGPP and FPP (10 μM) for 6 hours, and *Gilz* mRNA levels were measured. mRNA expression was normalized to the housekeeping gene (*Csnk2a2*) and is presented as fold change of control. Data show the mean of 2 (A, C2C12 data) or 3 (A, human myoblast data and B-E) independent experiments performed in replicates ± SEM. $^{**}P < .01$, $^{***}P < .001$ relative to the corresponding control, $^{++}P < .01$, $^{+++}P < .001$ relative to other treatments as indicated

(WT) and GILZ knockout (KO) mice, treated them with increasing doses of statins, and measured cell viability after 24 hours. Comparison of the dose-response curves obtained showed significant differences between genotypes: GILZ KO myoblasts were significantly less sensitive toward atorvastatin, simvastatin, and cerivastatin treatment than their WT counterparts (Figure 4A).

Due to the importance of the PI3K/Akt signaling pathway in statin-induced myotoxicity,[40,42] we hypothesized that the resistance to cell death from GILZ KO myoblasts might be related to modulation of the Akt phosphorylation status. Indeed, atorvastatin treatment induced dephosphorylation of Akt and activated the apoptotic pathway, as observed by cleaved caspase-3 detection, in WT myoblasts. On the other hand, Akt phosphorylation levels were restored to that of the control in statin-treated GILZ KO cells, and the active form of caspase-3 was undetectable (Figure 4B,C).

As an ex vivo model for the evaluation of statin myotoxicity, we used *flexor digitorum brevis* myofibers isolated from WT and KO animals. These short fibers can be isolated, dissociated, and cultured, representing a more mature system for evaluation of statin effects than cell culture systems, since myoblasts in

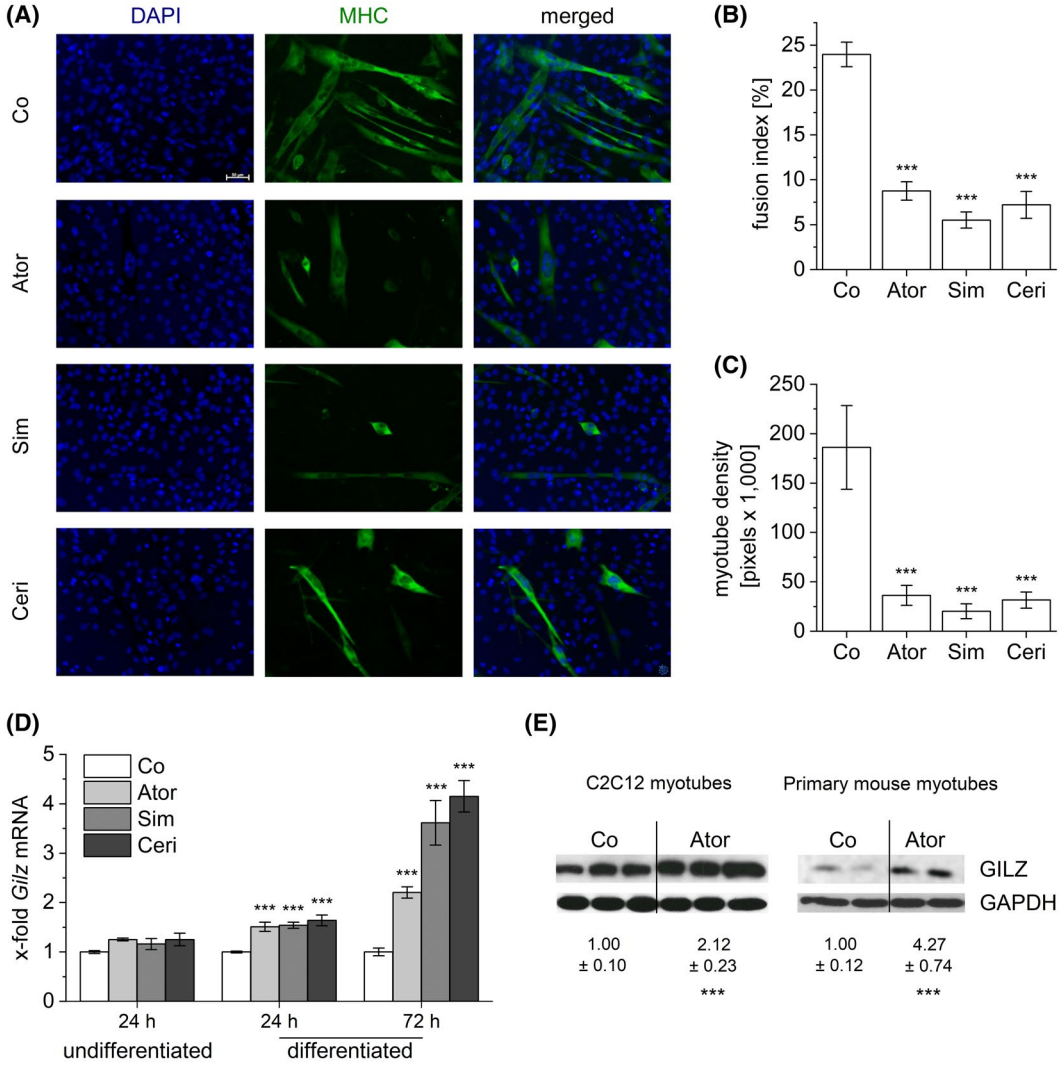

FIGURE 3 Effect of statins on GILZ expression during C2C12 differentiation. A-B, C2C12 were induced to differentiate for 6 days in the absence or presence of nontoxic concentrations of atorvastatin (5 μM), simvastatin (1 μM), and cerivastatin (0.1 μM), and subjected to MHC IF. Co: vehicle-treated cells. A, Representative images are shown. Blue: DAPI, green: MHC, scale bar: 50 μm. B, The degree of differentiation was quantified by measuring the fusion index in IF images. C, Myotube density in Jenner-Giemsa stained cells. D, *Gilz* expression was measured in nondifferentiated cells or cells differentiated for the indicated time points and normalized against the housekeeping gene (*Csnk2a2*). Data are presented as fold change of the corresponding vehicle-treated control (Co). E, GILZ protein levels measured in 72 h-C2C12 myotubes and primary murine myotubes treated with atorvastatin (5 μM) during the course of myogenesis. Representative blots are shown. Data represent the means of three independent experiments performed in replicates ± SEM. $^{*}P < .05$, $^{**}P < .01$, $^{***}P < .001$ relative to the control

vitro can differentiate to myotubes but are unable to form fully differentiated myocytes and, therefore, do not exactly resemble the features of mature muscle.[48,49] Treatment of FDB fibers from WT mice with atorvastatin, simvastatin, and cerivastatin started to induce vacuolation at 72 hours. After 5 days, the fibers were swollen, ruptured, and blebs appeared (Figure 5A and data not shown). Viability analysis using the trypan blue exclusion method after 5 days indicated that statins induced fiber death in a dose-dependent manner. Loss of GILZ prevented the morphological changes indicative of myotoxicity and made the fibers resistant toward statins: in KO fibers, there were no significant differences in viability between the control and treatments at any of the concentrations evaluated (Figure 5A,B).

3.6 | GILZ contributes to statin-induced inhibition of myogenesis

To investigate the contribution of GILZ to statin-induced inhibition of myogenesis, we differentiated WT and GILZ KO myoblasts in the presence of statins and evaluated the expression of the MRF myogenin, which is required in cells committed

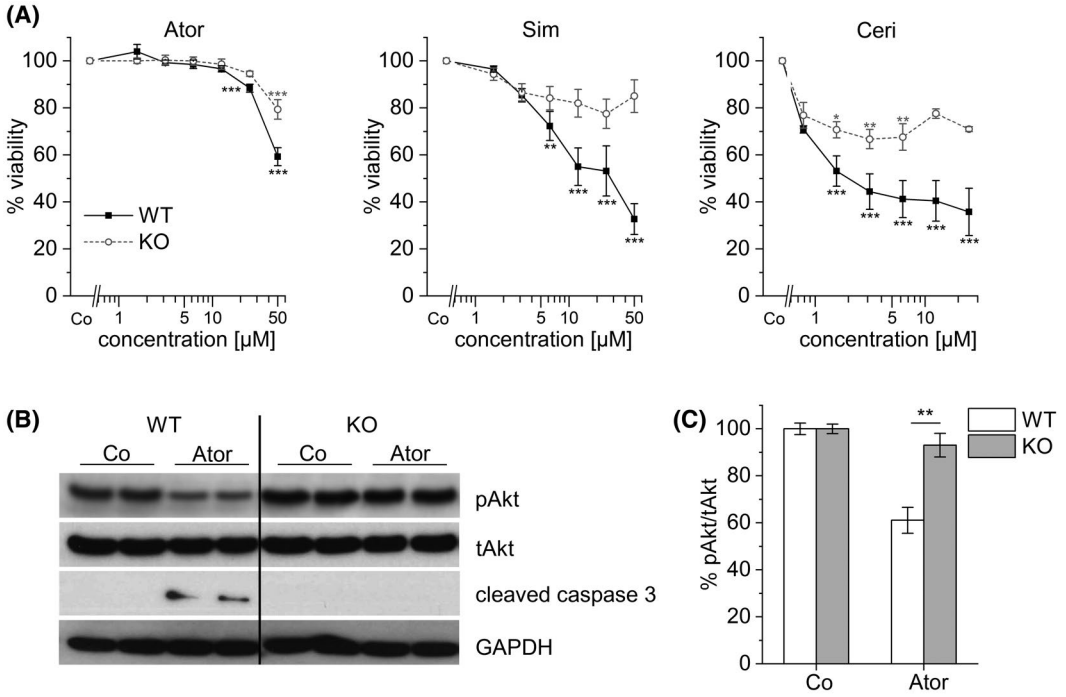

FIGURE 4 Effect of GILZ knockout on statin-induced myotoxicity. A, WT and GILZ KO primary murine myoblasts were treated with atorvastatin, simvastatin, or cerivastatin in increasing concentrations for 24 hours. Cell viability was measured via MTT assay and differences between curves were analyzed by two-way ANOVA [cell type main effect $F(1,124) = 10.06$, $P = .002$; $F(1,124) = 26.24$, $P < .0001$; and $F(1,116) = 24.18$, $P < .0001$, respectively, for each statin]. B, Myoblasts were treated with atorvastatin (50 μM) for 6 hours, and Akt phosphorylation and caspase-3 activation were measured by western blot. One representative blot is shown. C, The ratio of phosphorylated to total Akt was measured by densitometric analysis and normalized to the corresponding control. Data show the mean of at least three independent experiments performed in replicates ± SEM. $*P < .05$, $**P < .01$, $***P < .001$ relative to the control

to the myogenic program for driving their fusion and terminal differentiation.[44] We observed a decrease in myogenin protein levels in WT primary murine myoblasts induced to differentiate for 72 hours in the presence of atorvastatin. By contrast, the expression of myogenin in atorvastatin-treated GILZ KO cells was restored to that of the control (Figure 6A).

To further analyze the role of GILZ in these effects, we generated C2C12 cell lines stably expressing scrambled or *Gilz* shRNA constructs by lentiviral transduction. The C2C12^{shGilz1} and C2C12^{shGilz2} cell lines showed a gene knockdown, whereas in the scrambled control cell line, C2C12^{scr}, *Gilz* expression was unaffected (Supplemental Figure 5A). Furthermore, statin-induced GILZ overexpression was inhibited in *Gilz* shRNA-expressing cells (Supplemental Figure 5B,C). We hypothesized that, as a result of restored myogenin expression, *Gilz* silencing should reinstate the ability of myoblasts to differentiate in the presence of statins. Noticeably, C2C12^{shGilz1} and C2C12^{shGilz2} cells displayed terminally differentiated myotubes already after 4 days in DM, whereas C2C12^{scr} cells were not fully differentiated yet (Figure 6B, left panels). GILZ knockdown, however, could only partially reverse the impairment in differentiation caused by statins: although Jenner-Giemsa staining showed myotube formation in the C2C12^{shGilz} lines (Supplemental Figure 6), these myosin-expressing cells were not differentiated to the same extent as the respective controls. Nevertheless, fusion index analysis showed improvement in myotube formation from C2C12^{shGilz} cells compared to the C2C12^{scr} line (Figure 6C).

3.7 | FOXO3 mediates GILZ induction by statins in muscle

In the search for potential upstream regulators of GILZ expression after statin treatment in muscle, we focused on the Forkhead Box O3 (FOXO3) protein. FOXO3 is a direct phosphorylation target of Akt, and our observations in skeletal muscle tissue from FOXO3 KO mice, where *Gilz* expression levels were significantly lower than in WT animals, hinted toward FOXO3 as a transcriptional regulator of GILZ in this tissue (Figure 7A). Reporter gene assay showed that statins were able to induce FOXO3 transcriptional activity (Supplemental Figure 7) and, in fact, led to increased *Gilz* promoter-driven luciferase activity in C2C12 compared to the baseline. This indicates that statins elevate GILZ levels by activating its transcription (Figure 7B). Like in primary myoblasts, we observed that treatment of C2C12 myoblasts with statins led

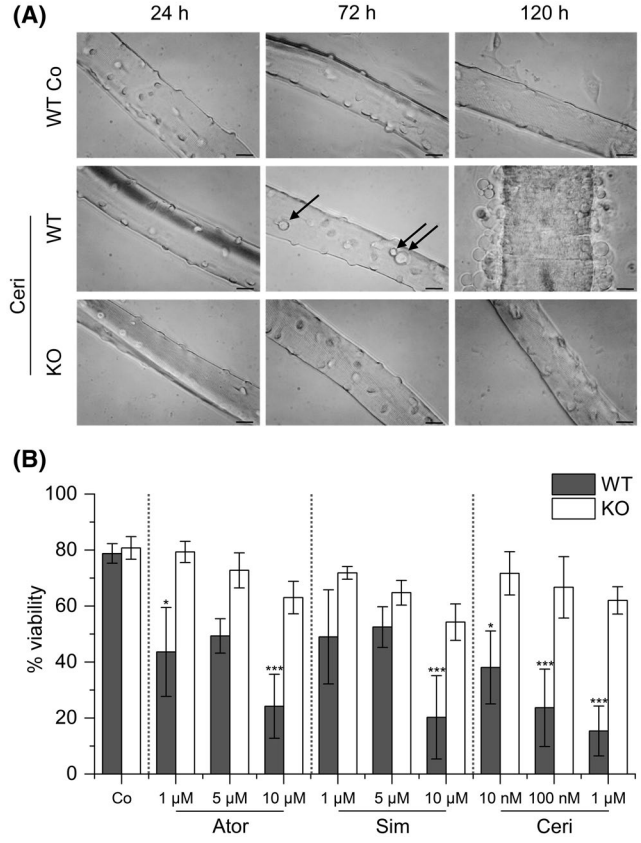

FIGURE 5 Effect of GILZ knockout on statin-induced FDB myofiber toxicity. WT and GILZ KO FDB myofibers were treated with cerivastatin (1 μM) for up to 120 hours and imaged for morphological analysis. A, Representative pictures are shown. Scale bar, 20 μm. B, Cell viability was measured after 120 hours of treatment, using the trypan blue exclusion method. Data show the mean of four independent experiments performed in replicates ± SEM. $*P < .05$, $***P < .001$ relative to the corresponding control

to a decrease in Akt phosphorylation and, in line with this, to reduced levels of phosphorylated FOXO3 protein, that is, FOXO3 activation in parallel to GILZ induction (Figure 7C-E). Hence, we performed chromatin immunoprecipitation to evaluate whether FOXO3 activated *Gilz* expression in myoblasts by binding to the forkhead-responsive elements (FHRE) in its promoter following statin treatment. Indeed, we found an enrichment of sequences corresponding to three of the four FHREs presents in the *Gilz* promoter in immunoprecipitates from atorvastatin-treated myoblasts, indicating that GILZ induction in muscle follows dephosphorylation, nuclear translocation, and activation of FOXO3 (Figure 7F).

3.8 | Statins induce Gilz in zebrafish embryos, and deregulation of Gilz expression impairs somitogenesis

The zebrafish is a powerful and versatile in vivo model for the study of developmental and physiological processes, that has been used for the elucidation of statin effects on muscle development[50] and homeostasis.[41,51,52] Given that the zebrafish expresses a GILZ orthologue,[53] we chose this model to study the effects of statins on GILZ expression in vivo adhering to 3R rules to reduce animal experiments.

In line with our in vitro findings, treatment of zebrafish embryos at 20 hpf with statins at concentrations that have been described to cause major muscle damage[34] led to an upregulation of *gilz* mRNA (Figure 8A). Moreover, statin treatment of embryos in the 2-4 cell stage for 24 hours resulted in disrupted muscle development in the tail of the embryos and a reduction of the frequency and dimension of muscle contractions, indicating an impaired muscle function (Figure 8B, Supplemental video). To characterize the effects of increased *gilz* expression in zebrafish muscle development, we performed myosin heavy chain IF and MyoD staining in *gilz* overexpressing and statin-treated embryos. Compared to control animals, we found an irregular MyoD expression and diffuse MHC staining with loss of septa in statin-treated embryos. Overexpression of *gilz* mimicked statin effects, suggesting that *gilz* mediated statin-induced muscle damage in this model (Figure 8C,D).

To investigate whether FOXO3b, the orthologue of mammalian FOXO3, was involved in *gilz* upregulation by statins, we knocked down *foxo3b* by morpholino injection.[35] *gilz* levels were reduced in *foxo3b* depleted embryos (Supplemental Figure 8). It was not possible to assess statin-induced muscle damage after morpholino-mediated knockdown of *foxo3b* because the embryos showed severe defects in axis formation, as previously reported by Xie et al[35] (Supplemental Figure 8B).

4 | DISCUSSION

More than 30 years after their introduction to the market, statins remain the cornerstone of the pharmacological management of hyperlipidemia and CVD prevention. In light of their importance and extended use, the understanding of the mechanisms underlying the onset of SAMS is of highest relevance.[10] In the present study, we report a role for GILZ as a pivotal mediator of the myotoxic and antimyogenic effects of statins. We first demonstrate that treatment of murine myoblasts with different statins, at concentrations typical for in vitro studies on SAMS,[41,43,54] induces GILZ expression. Since SAMS are a class effect and several of the mechanisms underlying muscle toxicity are directly related to the inhibition of HMG-CoA,[47,55] we evaluated whether GILZ expression depended on this pathway as well. Indeed, we found GILZ induction to depend on mevalonate, and more specifically on geranylgeranylation.[34]

Several molecular mechanisms of statin-induced myotoxicity have been proposed, describing their deleterious effects

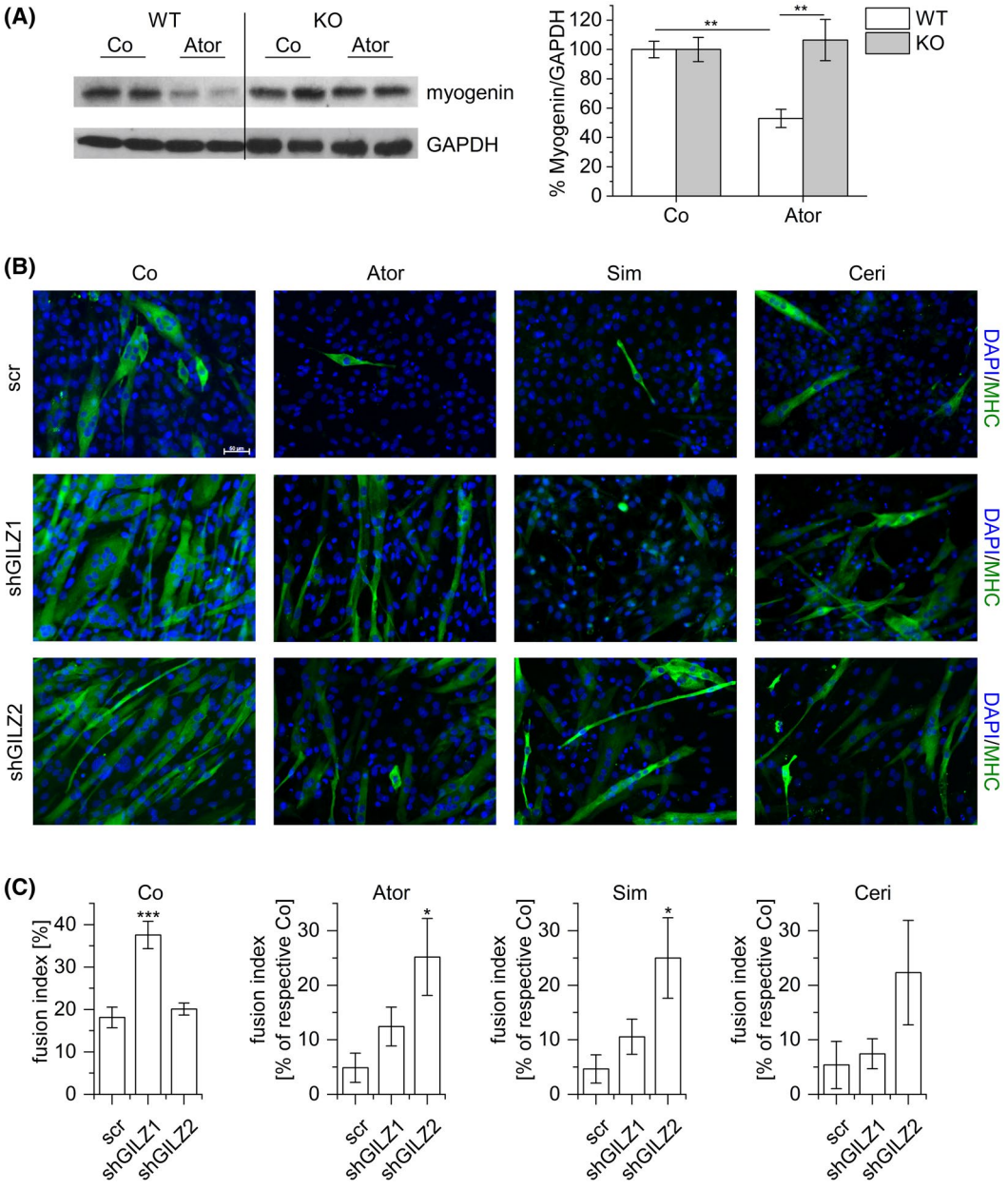

FIGURE 6 Effect of GILZ absence on statin-induced antimyogenic effects. A, Primary murine myoblasts from GILZ WT and KO animals were differentiated for 72 hours in the absence or presence of atorvastatin (5 μM). Myogenin protein levels were measured by western blot. One representative blot and the densitometric analysis are shown. B-C, Scrambled ($C2C12^{scr}$) and $C2C12^{shGILZ}$ cell lines were induced to differentiate for 4 days in the absence or presence of atorvastatin (5 μM), simvastatin (1 μM), and cerivastatin (0.1 μM). Co: vehicle-treated cells. B, MHC IF. Blue: DAPI, green: MHC, scale bar: 50 μm. Representative images are shown. C, The degrees of differentiation was quantified by measuring the fusion index. For statin-treated cells the fusion index is expressed as percentage of the corresponding vehicle-treated control. Data show the mean of at least three independent experiments performed in replicates ± SEM. $*P < .05$, $**P < .01$, $***P < .001$ relative to the equally treated scr cells (C) or as indicated (A)

on mitochondrial function, calcium homeostasis, and cell survival in the myocyte.[14] In our hands, statins caused Akt dephosphorylation and activation of the apoptotic cascade in undifferentiated myoblasts. This effect is in accordance with previous findings in cultured myotubes.[42,56] Our observations suggest a crucial role for GILZ in mediating this action. First described in thymocytes as an antiapoptotic protein,[15] GILZ can exert anti- or pro-apoptotic effects depending on the cell type: GILZ has been shown to promote apoptosis by Mcl-1 downregulation in neutrophils[57] and by inhibition of the Akt/mTOR signaling pathway in myeloma cells.[58]

There are discrepancies, however, regarding the mechanism by which statins induce cell death in cultured myoblasts/myotubes *vs.* mature fibers. For instance, statins trigger apoptosis in cultured cells, whereas mature skeletal muscles show necrotic features.[49] Hence, instead of using terminally

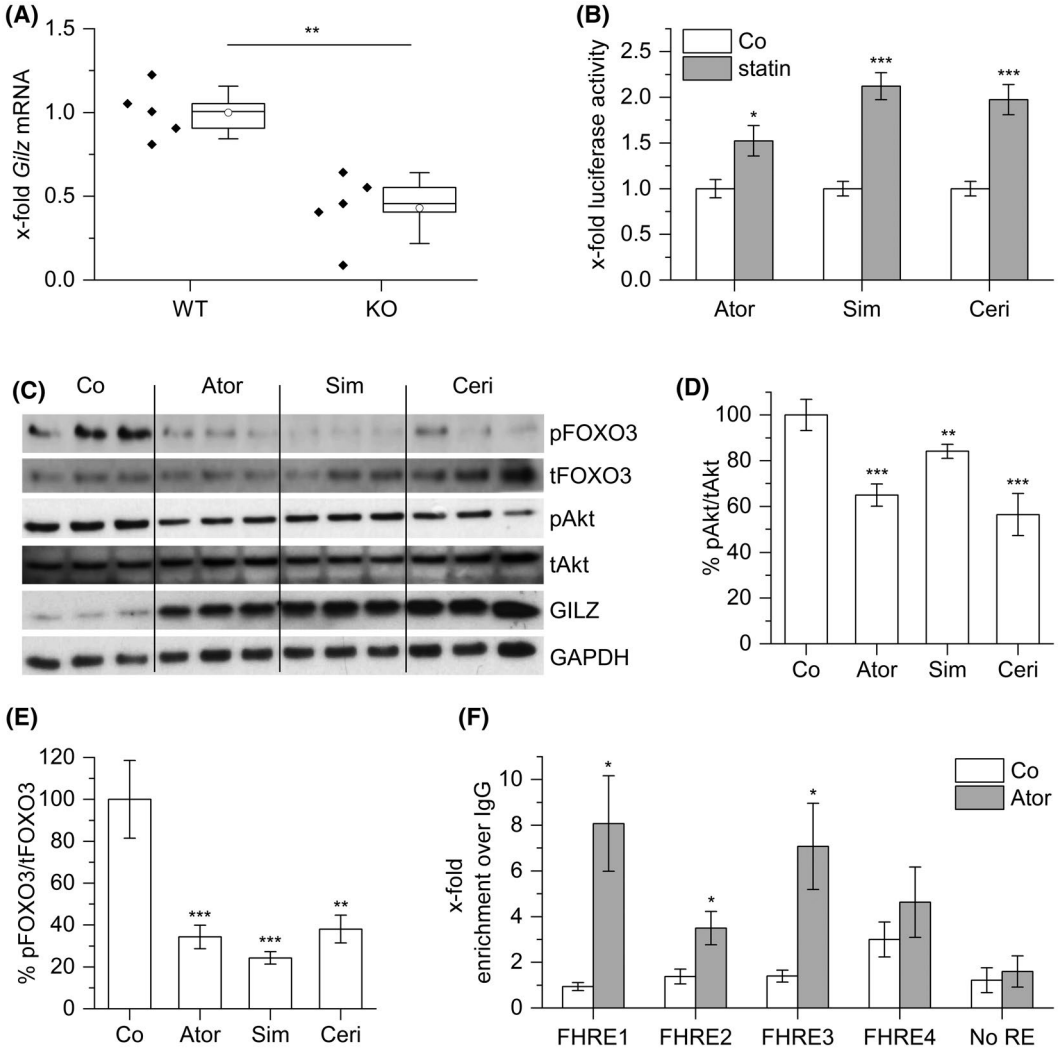

FIGURE 7 Involvement of FOXO3 in statin-induced GILZ expression. A, *Gilz* expression on skeletal muscle from WT and FOXO3 KO mice (n = 5). mRNA expression data normalized against the housekeeping gene (*Csnk2a2*) and is presented as fold change of WT in boxplots showing the 25-75th percentiles, mean (square), median (line), and SD (whiskers). B, Reporter gene assay in C2C12 myoblasts transfected with a *Gilz* promoter reporter plasmid and treated with vehicle (Co) or statins (50 μM) for 6 hours. Luciferase activity was normalized to the vehicle-treated control. C-E, Western blot analysis of statin-treated C2C12 cells (50 μM, 6 hours; Co: vehicle control). C, One representative blot is shown. D-E, Densitometric analysis. Values for vehicle-treated controls were set as 1. F, ChIP analysis was used to detect the binding of FOXO3 to the *Gilz* promoter region. Data are presented as fold enrichment over IgG. Data show the mean of at least three independent experiments performed in replicates ± SEM. **P* < .05, **P < .01, ****P* < .001 relative to the vehicle-treated control

differentiated cultured myotubes, we chose isolated FDB myofibers as an *ex vivo* model to evaluate the effects of the absence of GILZ in statin toxicity toward mature muscle. We noticed that treatment of murine FDB fibers with atorvastatin, simvastatin, and cerivastatin caused cell death with similar features as those previously described for fluvastatin-treated rat FDB fibers.[59] Furthermore, in accordance with our observations in proliferating myoblasts, GILZ was of crucial importance in mediating statin-induced fiber breakdown.

FOXO3 is a transcription factor involved in different aspects of muscle homeostasis, like regulation of mitochondrial metabolism, activation of protein breakdown *via* the ubiquitin-proteasome and autophagy pathways, and inhibition of muscle precursor cell proliferation.[60] In statin-induced myopathy, reports have shown that FOXO3 activation results in expression of the muscle atrophy-related protein MAFbx/atrogin-1 and other genes implicated in muscle proteolysis in vitro and in vivo.[40,41] Moreover, FOXO3 has been reported as a transcriptional regulator of GILZ in T cells, where it drives IL-2 withdrawal-induced GILZ expression.[61] We found statin-induced GILZ expression in muscle to be FOXO3-dependent and, as mentioned above, GGPP dependent. These results are in accordance with previous studies that linked SAMS to reduced geranylgeranylation, but not farnesylation of different small GTPases like Rac1, Rap1, and Rab1.[34,45,56,62] Our findings suggest that the inhibition of protein geranylgeranylation by statins downregulates the

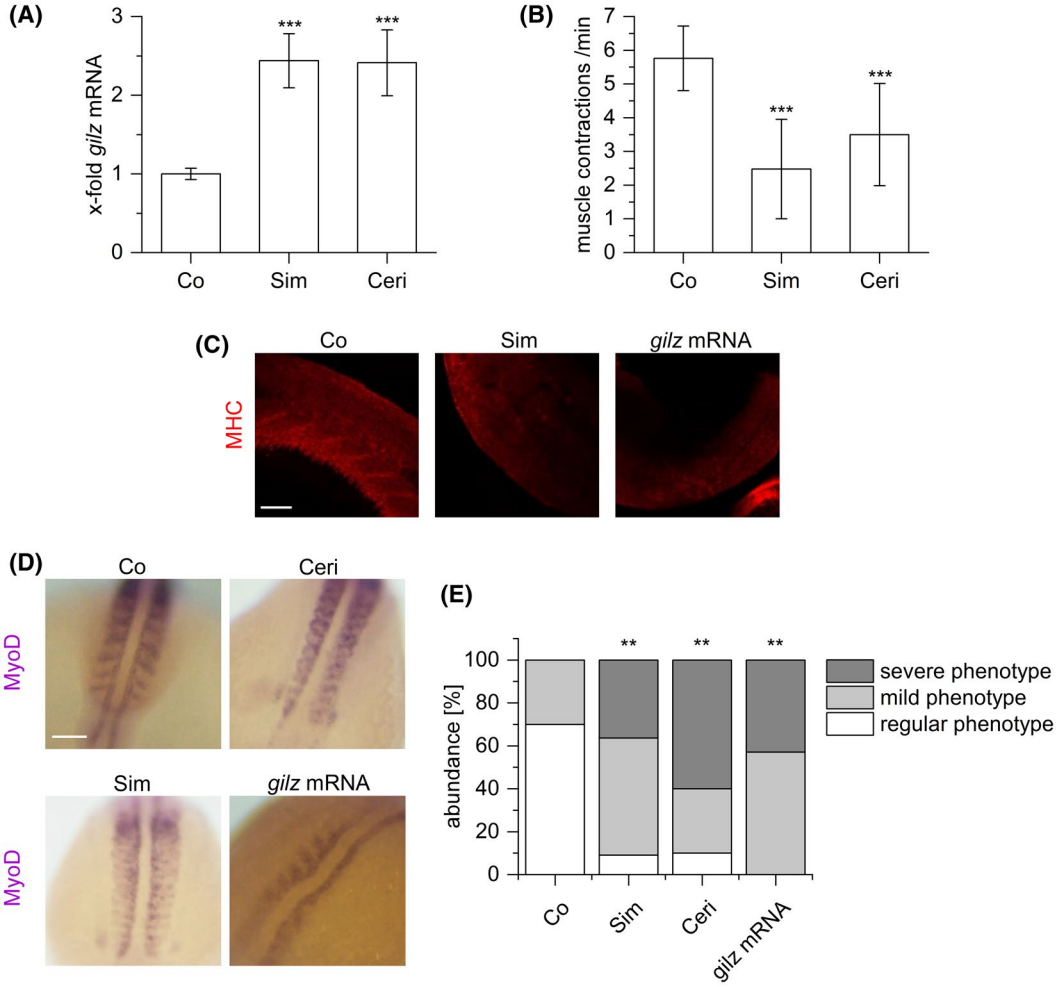

FIGURE 8 Effects of statins and GILZ on zebrafish muscle development. A, Zebrafish embryos at 20 hpf were treated with simvastatin lactone (1 μM) or cerivastatin (1 μM) for 12 hours. mRNA expression was normalized to the housekeeping gene (*actb2*) and is presented as fold change of control ± SEM (n = 3, duplicates). B, Zebrafish embryos at the 1-2 cell stage were treated with simvastatin lactone (1 μM) or cerivastatin (1 μM) for 24 hours, and muscle contractions per minute were counted (n ≥ 10) and are presented as means ± SEM. C-D, 1 ng statin or vehicle (Co) were injected into zebrafish embryos in the 1-2 cell stage. C, MHC IF of statin-treated and *gilz*-overexpressing 24 hpf embryos. Representative images are shown. A diffuse staining and a complete loss of the V-shaped somite pattern was observed in all simvastatin- or *gilz* mRNA-treated embryos (n ≥ 10 per group). Panels are side views. Red: MHC, scale bar: 50 μm. D, MyoD in situ hybridization of statin treated and *gilz*-overexpressing 16 hpf embryos shows a severely impaired MyoD expression when compared to control. Representative images are shown. Panels are dorsal views. Violet: MyoD, scale bar: 60 μm. E: Phenotypic scoring of MyoD-stained embryos (n = 7-10 per group). **P* < .05, ***P* < .01, ****P* < .001, relative to the control

Akt signaling pathway, leading to FOXO3-driven GILZ induction, which in turn further decreases Akt phosphorylation and promotes apoptosis of muscle cells.

The fact that GILZ is expressed in skeletal muscle, as observed by us and reported in earlier studies,[16] might denote a role in muscle tissue homeostasis. Indeed, an earlier study showed that GILZ and its longer isoform, L-GILZ, modulate myogenesis in the absence of pharmacological intervention, and mediate glucocorticoid-induced inhibition of myogenesis by decreasing MyoD-mediated myogenin transcription, thus impairing myoblast fusion.[22] For this reason, we investigated the role of GILZ in the antimyogenic effects of statins and found that the degree of GILZ induction during myogenesis was correlated to the antimyogenic effect of the statin used. A previous study reported no differences in myogenin mRNA levels in simvastatin-treated C2C12.[45] We, however, found myogenin protein expression to be impaired in primary differentiating myoblasts treated with atorvastatin. Moreover, our results in GILZ KO myoblasts indicate that statin-induced GILZ expression, and the consequent myogenin transcriptional repression, is a mechanism by which this class of drugs impairs myogenesis.

GILZ silencing by shRNA caused the resulting C2C12^{shGilz} cell lines to differentiate considerably faster than the C2C12^{scr} control, even to a higher degree than observed for WT cells after terminal differentiation. This supports the importance

of GILZ itself as a modulator of myogenesis and corresponds to our observations in zebrafish embryos, where *gilz* overexpression severely impaired somitogenesis. Importantly, zebrafish embryos represent a frequently used in vivo model for the mechanistic study of SAMS.[50-52,63] The regulatory role played by GILZ in zebrafish embryonic development is rather complex: the study that first described the presence of a GILZ orthologue in zebrafish showed that manipulation of *gilz* expression in this model, either *via* morpholino oligomer silencing or mRNA overexpression, causes significant defects in embryonic development, altering the dorsoventral patterning, segmentation, and brain development processes.[53] In rodents, however, GILZ-independent regulatory pathways are most likely involved in the modulation of skeletal muscle development, since GILZ KO mice do not exhibit altered muscle features (unpublished observations).

Even though myogenin expression was rescued in the absence of GILZ, we could not observe a complete recovery in myotube formation after statin treatment in C2C12^{shGilz} cells. This might be related to residual GILZ expression in the silenced cells, or to additional pathways that mediate the antimyogenic effects observed, such as the IGF-1/PI3K/Akt pathway.[46] Our observations indicate that GILZ is critical for statin-induced inhibition of myogenin, an MRF crucial for myoblast fusion and terminal differentiation.[64] Additional factors, however, may also contribute to the inhibition of muscle regeneration by statins.

Taken together, our data point toward GILZ as an essential mediator of the molecular mechanisms leading to statin-induced muscle damage and impairment of muscle regeneration. This study contributes to a better understanding of the molecular mechanisms underlying statin-induced myopathy, a necessary step toward the development of prevention strategies, and safer therapy approaches for a class of drugs that remains a pillar in the treatment of cardiovascular disease.

CONFLICT OF INTEREST

The authors have nothing to disclose.

AUTHORS CONTRIBUTIONS

J. Hoppstädter, J.V. Valbuena Perez, R. Linnenberger, C. Dahlem, A. Hecksteden, W.K.F. Tse, S. Bruscoli, and S. Flamini conducted experiments. J.V. Valbuena Perez, J. Hoppstädter, R. Linnenberger, T.M. Legroux, and C. Dahlem acquired and analyzed data. J.V. Valbuena Perez, J. Hoppstädter, A.K. Kiemer, and R. Linnenberger wrote the manuscript. A. Andreas, J. Herrmann, C. Herr, S. Bruscoli, and W.K.F. Tse supported the mouse and zebrafish experiments. S. Bruscoli, C. Riccardi, A.K. Kiemer, and J. Hoppstädter designed research studies. J. Herrmann, R. Müller, R. Bals, C. Riccardi, S. Bruscoli, A.K. Kiemer, A. Hecksteden, and J. Hoppstädter supervised the experiments, and all authors revised the manuscript. AKK initiated the study.

REFERENCES

1. Grundy SM, Stone NJ, Bailey AL, et al. 2018 AHA/ACC/AACVPR/AAPA/ABC/ACPM/ADA/AGS/APhA/ASPC/NLA/PCNA guideline on the management of blood cholesterol: a report of the American College of Cardiology/American Heart Association task force on clinical practice guidelines. *Circulation*. 2019;139:e1082-e1143.
2. Catapano AL, Graham I, De Backer G, et al. 2016 ESC/EAS guidelines for the management of dyslipidaemias. *Eur Heart J*. 2016;37:2999-3058.
3. Sirtori CR. The pharmacology of statins. *Pharmacol Res*. 2014;88:3-11.
4. Ward NC, Watts GF, Eckel RH. Statin toxicity. *Circ Res*. 2019;124:328-350.
5. Vancheri F, Backlund L, Strender LE, Godman B, Wettermark B. Time trends in statin utilisation and coronary mortality in Western European countries. *BMJ Open*. 2016;6:e010500.
6. Salami JA, Warraich H, Valero-Elizondo J, et al. National trends in statin use and expenditures in the US adult population from 2002 to 2013: insights from the medical expenditure panel survey. *JAMA Cardiol*. 2017;2:56-65.
7. Nolte E, Newbould J, Conklin A. International variation in the usage of medicines: a review of the literature. *Rand Health Q*. 2011;1:4.
8. Taylor F, Huffman MD, Macedo AF, et al. Statins for the primary prevention of cardiovascular disease. *Cochrane Database Syst Rev*. 2013;CD004816.
9. Heller DJ, Coxson PG, Penko J, et al. Evaluating the impact and cost-effectiveness of statin use guidelines for primary prevention of coronary heart disease and stroke. *Circulation*. 2017;136:1087-1098.
10. Stroes ES, Thompson PD, Corsini A, et al. Statin-associated muscle symptoms: impact on statin therapy-European atherosclerosis society consensus panel statement on assessment, aetiology and management. *Eur Heart J*. 2015;36:1012-1022.
11. Mosshammer D, Schaeffeler E, Schwab M, Morike K. Mechanisms and assessment of statin-related muscular adverse effects. *Br J Clin Pharmacol*. 2014;78:454-466.
12. Laufs U, Filipiak KJ, Gouni-Berthold I, Catapano AL, Mandraffino G, Benlian P. Practical aspects in the management of statin-associated muscle symptoms (SAMS). *Atheroscler Suppl*. 2017;26:45-55.
13. Needham M, Mastaglia FL. Statin myotoxicity: a review of genetic susceptibility factors. *Neuromuscul Disord*. 2014;24:4-15.
14. du Souich P, Roederer G, Dufour R. Myotoxicity of statins: mechanism of action. *Pharmacol Ther*. 2017;175:1-16.
15. D'Adamio F, Zollo O, Moraca R, et al. A new dexamethasone-induced gene of the leucine zipper family protects T lymphocytes from TCR/CD3-activated cell death. *Immunity*. 1997;7:803-812.
16. Cannarile L, Zollo O, D'Adamio F, et al. Cloning, chromosomal assignment and tissue distribution of human GILZ, a glucocorticoid hormone-induced gene. *Cell Death Differ*. 2001;8:201-203.
17. Bereshchenko O, Migliorati G, Bruscoli S, Riccardi C. Glucocorticoid-induced leucine zipper: a novel anti-inflammatory molecule. *Front Pharmacol*. 2019;10:305.

18. Shi X, Shi W, Li Q, et al. A glucocorticoid-induced leucine-zipper protein, GILZ, inhibits adipogenesis of mesenchymal cells. *EMBO Rep*. 2003;4:374-380.
19. Soundararajan R, Zhang TT, Wang J, Vandewalle A, Pearce D. A novel role for glucocorticoid-induced leucine zipper protein in epithelial sodium channel-mediated sodium transport. *J Biol Chem*. 2005;280:39970-39981.
20. Rashmi P, Colussi G, Ng M, Wu X, Kidwai A, Pearce D. Glucocorticoid-induced leucine zipper protein regulates sodium and potassium balance in the distal nephron. *Kidney Int*. 2017;91:1159--1177.
21. Bruscoli S, Velardi E, Di Sante M, et al. Long glucocorticoid-induced leucine zipper (L-GILZ) protein interacts with ras protein pathway and contributes to spermatogenesis control. *J Biol Chem*. 2012;287:1242-1251.
22. Bruscoli S, Donato V, Velardi E, et al. Glucocorticoid-induced leucine zipper (GILZ) and long GILZ inhibit myogenic differentiation and mediate anti-myogenic effects of glucocorticoids. *J Biol Chem*. 2010;285:10385-10396.
23. Keire P, Shearer A, Shefer G, Yablonka-Reuveni Z. Isolation and culture of skeletal muscle myofibers as a means to analyze satellite cells. *Methods Mol Biol*. 2013;946:431-468.
24. Park KH, Weisleder N, Zhou J, et al. Assessment of calcium sparks in intact skeletal muscle fibers. *J Vis Exp*. 2014;e50898.
25. Hoppstädter J, Hachenthal N, Valbuena-Perez JV, et al. Induction of glucocorticoid-induced leucine zipper (GILZ) contributes to anti-inflammatory effects of the natural product curcumin in macrophages. *J Biol Chem*. 2016;291:22949-22960.
26. Czepukojc B, Abuhaliema A, Bargash A, et al. *IGF2* mRNA binding protein 2 transgenic mice are more prone to develop a ductular reaction and to progress toward cirrhosis. *Front Med*. 2019;6:179.
27. Bruscoli S, Sorcini D, Flamini S, et al. Glucocorticoid-induced leucine zipper inhibits interferon-gamma production in B Cells and suppresses colitis in mice. *Front Immunol*. 2018;9:1720.
28. Hoppstädter J, Diesel B, Linnenberger R, et al. Amplified host defense by Toll-like receptor-mediated downregulation of the glucocorticoid-induced leucine zipper (GILZ) in macrophages. *Front Immunol*. 2019;9:3111.
29. Hoppstädter J, Dembek A, Linnenberger R, et al. Toll-like receptor 2 release by macrophages: an anti-inflammatory program induced by glucocorticoids and lipopolysaccharide. *Front Immunol*. 2019;10:1634.
30. Velica P, Bunce CM. A quick, simple and unbiased method to quantify C2C12 myogenic differentiation. *Muscle Nerve*. 2011;44:366-370.
31. Schindelin J, Arganda-Carreras I, Frise E, et al. Fiji: an open-source platform for biological-image analysis. *Nat Methods*. 2012;9:676-682.
32. Andres V, Walsh K. Myogenin expression, cell cycle withdrawal, and phenotypic differentiation are temporally separable events that precede cell fusion upon myogenesis. *J Cell Biol*. 1996;132:657-666.
33. Kimmel CB, Ballard WW, Kimmel SR, Ullmann B, Schilling TF. Stages of embryonic development of the zebrafish. *Dev Dyn*. 1995;203:253-310.
34. Cao P, Hanai J, Tanksale P, Imamura S, Sukhatme VP, Lecker SH. Statin-induced muscle damage and atrogin-1 induction is the result of a geranylgeranylation defect. *FASEB J*. 2009;23:2844-2854.
35. Xie XW, Liu JX, Hu B, Xiao W. Zebrafish foxo3b negatively regulates canonical Wnt signaling to affect early embryogenesis. *PLoS ONE*. 2011;6:e24469.
36. Brunet A, Bonni A, Zigmond MJ, et al. Akt promotes cell survival by phosphorylating and inhibiting a Forkhead transcription factor. *Cell*. 1999;96:857-868.
37. Moffat J, Grueneberg DA, Yang X, et al. A lentiviral RNAi library for human and mouse genes applied to an arrayed viral high-content screen. *Cell*. 2006;124:1283-1298.
38. Sarbassov DD, Guertin DA, Ali SM, Sabatini DM. Phosphorylation and regulation of Akt/PKB by the rictor-mTOR complex. *Science*. 2005;307:1098-1101.
39. Laaksonen R, Katajamaa M, Paiva H, et al. A systems biology strategy reveals biological pathways and plasma biomarker candidates for potentially toxic statin-induced changes in muscle. *PLoS ONE*. 2006;1:e97.
40. Mallinson JE, Constantin-Teodosiu D, Sidaway J, Westwood FR, Greenhaff PL. Blunted Akt/FOXO signalling and activation of genes controlling atrophy and fuel use in statin myopathy. *J Physiol*. 2009;587:219-230.
41. Hanai J, Cao P, Tanksale P, et al. The muscle-specific ubiquitin ligase atrogin-1/MAFbx mediates statin-induced muscle toxicity. *J Clin Invest*. 2007;117:3940-3951.
42. Bonifacio A, Sanvee GM, Bouitbir J, Krahenbuhl S. The AKT/mTOR signaling pathway plays a key role in statin-induced myotoxicity. *Biochim Biophys Acta*. 2015;1853:1841-1849.
43. Schirris TJ, Renkema GH, Ritschel T, et al. Statin-induced myopathy is associated with mitochondrial complex III inhibition. *Cell Metab*. 2015;22:399-407.
44. Bentzinger CF, Wang YX, Rudnicki MA. Building muscle: molecular regulation of myogenesis. *Cold Spring Harb Perspect Biol*. 2012;4:a008342.
45. Baba TT, Nemoto TK, Miyazaki T, Oida S. Simvastatin suppresses the differentiation of C2C12 myoblast cells via a Rac pathway. *J Muscle Res Cell Motil*. 2008;29:127-134.
46. Ogura T, Tanaka Y, Nakata T, Namikawa T, Kataoka H, Ohtsubo Y. Simvastatin reduces insulin-like growth factor-1 signaling in differentiating C2C12 mouse myoblast cells in an HMG-CoA reductase inhibition-independent manner. *J Toxicol Sci*. 2007;32:57-67.
47. Trapani L, Segatto M, La Rosa P, et al. 3-hydroxy 3-methylglutaryl coenzyme a reductase inhibition impairs muscle regeneration. *J Cell Biochem*. 2012;113:2057-2063.
48. Ravenscroft G, Nowak KJ, Jackaman C, et al. Dissociated flexor digitorum brevis myofiber culture system-a more mature muscle culture system. *Cell Motil Cytoskeleton*. 2007;64:727-738.
49. Sakamoto K, Kimura J. Mechanism of statin-induced rhabdomyolysis. *J Pharmacol Sci*. 2013;123:289-294.
50. Campos LM, Rios EA, Guapyassu L, et al. Alterations in zebrafish development induced by simvastatin: comprehensive morphological and physiological study, focusing on muscle. *Exp Biol Med (Maywood)*. 2016;241:1950-1960.
51. Pasha R, Moon TW. Coenzyme Q10 protects against statin-induced myotoxicity in zebrafish larvae (Danio rerio). *Environ Toxicol Pharmacol*. 2017;52:150-160.
52. Huang SH, Hsiao CD, Lin DS, Chow CY, Chang CJ, Liau I. Imaging of zebrafish in vivo with second-harmonic generation reveals shortened sarcomeres associated with myopathy induced by statin. *PLoS ONE*. 2011;6:e24764.
53. Tse WK, Jiang YJ, Wong CK. Zebrafish transforming growth factor-beta-stimulated clone 22 domain 3 (TSC22D3) plays critical roles in Bmp-dependent dorsoventral patterning via two deubiquitylating enzymes Usp15 and Otud4. *Biochim Biophys Acta*. 2013;1830:4584-4593.

54. Bouitbir J, Charles AL, Echaniz-Laguna A, et al. Opposite effects of statins on mitochondria of cardiac and skeletal muscles: a 'mitohormesis' mechanism involving reactive oxygen species and PGC-1. *Eur Heart J*. 2012;33:1397-1407.
55. Osaki Y, Nakagawa Y, Miyahara S, et al. Skeletal muscle-specific HMG-CoA reductase knockout mice exhibit rhabdomyolysis: a model for statin-induced myopathy. *Biochem Biophys Res Commun*. 2015;466:536-540.
56. Johnson TE, Zhang X, Bleicher KB, et al. Statins induce apoptosis in rat and human myotube cultures by inhibiting protein geranylgeranylation but not ubiquinone. *Toxicol Appl Pharmacol*. 2004;200:237-250.
57. Espinasse MA, Pepin A, Virault-Rocroy P, et al. Glucocorticoid-induced leucine zipper is expressed in human neutrophils and promotes apoptosis through Mcl-1 down-regulation. *J Innate Immun*. 2016;8:81-96.
58. Joha S, Nugues AL, Hetuin D, et al. GILZ inhibits the mTORC2/AKT pathway in BCR-ABL(+) cells. *Oncogene*. 2012;31:1419-1430.
59. Sakamoto K, Wada I, Kimura J. Inhibition of Rab1 GTPase and endoplasmic reticulum-to-Golgi trafficking underlies statin's toxicity in rat skeletal myofibers. *J Pharmacol Exp Ther*. 2011;338:62-69.
60. Sanchez AM, Candau RB, Bernardi H. FoxO transcription factors: their roles in the maintenance of skeletal muscle homeostasis. *Cell Mol Life Sci*. 2014;71:1657-1671.
61. Asselin-Labat ML, Biola-Vidamment A, Kerbrat S, Lombes M, Bertoglio J, Pallardy M. FoxO3 mediates antagonistic effects of glucocorticoids and interleukin-2 on glucocorticoid-induced leucine zipper expression. *Mol Endocrinol*. 2005;19:1752-1764.
62. Sakamoto K, Honda T, Yokoya S, Waguri S, Kimura J. Rab-small GTPases are involved in fluvastatin and pravastatin-induced vacuolation in rat skeletal myofibers. *FASEB J*. 2007;21:4087-4094.
63. Campos LM, Rios EA, Midlej V, et al. Structural analysis of alterations in zebrafish muscle differentiation induced by simvastatin and their recovery with cholesterol. *J Histochem Cytochem*. 2015;63:427-437.
64. Asfour HA, Allouh MZ, Said RS. Myogenic regulatory factors: the orchestrators of myogenesis after 30 years of discovery. *Exp Biol Med (Maywood)*. 2018;243:118-128.

SUPPORTING INFORMATION

Additional supporting information may be found online in the Supporting Information section.

How to cite this article: Hoppstädter J, Valbuena Perez JV, Linnenberger R, et al. The glucocorticoid-induced leucine zipper mediates statin-induced muscle damage. *The FASEB Journal*. 2020;34:4684–4701. https://doi.org/10.1096/fj.201902557RRR